The role of shallow traps in dynamic characterization of organic semiconductor devices

Evelyne Knapp and Beat Ruhstaller

Citation: J. Appl. Phys. **112**, 024519 (2012); doi: 10.1063/1.4739303
View online: http://dx.doi.org/10.1063/1.4739303
View Table of Contents: http://jap.aip.org/resource/1/JAPIAU/v112/i2
Published by the American Institute of Physics.

The role of shallow traps in dynamic characterization of organic semiconductor devices

Evelyne Knapp[1,a)] and Beat Ruhstaller[1,2,b)]
[1]*Institute of Computational Physics, Zurich University of Applied Sciences, Wildbachstr. 21, 8401 Winterthur, Switzerland*
[2]*Fluxim AG, Dorfstrasse 7, 8835 Feusisberg, Switzerland*

(Received 15 March 2012; accepted 27 June 2012; published online 31 July 2012)

We present an analysis of charge mobility determination methods for the steady as well as the transient state and investigate shallow charge traps with respect to their dynamic behavior. We distinguish between fast and slow trap states in our numerical model corresponding to two characteristic regimes. The two regimes manifest themselves in both impedance spectroscopy and dark injection transient currents (DITC). Further we investigate the charge mobility obtained from dynamic simulations and relate it to the extracted charge mobility from steady-state current-voltage curves. To demonstrate the practical impact of these regimes, we apply our numerical model to the DITC that have commonly been used to determine the charge mobility in organic semiconductor devices. The obtained results from DITC studies strongly depend on the measurement conditions. Therefore we analyze the measurements of reference [Esward *et al.*, J. Appl. Phys. **109**, 093707 (2011)] and reproduce the effects of varying pulse off-times on the transient current qualitatively. Thus, our simulations are able to explain the experimental observations with the help of relaxation effects due to shallow traps. © *2012 American Institute of Physics*. [http://dx.doi.org/10.1063/1.4739303]

I. INTRODUCTION

The determination of the charge mobility in organic semiconductor devices is a crucial step in understanding and optimizing the devices. Different measurement and charge mobility extraction methods have been used in the steady as well as in the transient state.[1–9] For the steady-state characterization, the extended Gaussian disorder model (EGDM)[10] has successfully been applied to model current voltage curves of single-carrier devices.[11,12] For transient measurements, various modeling approaches are suggested by Refs. 13–17. The steady-state EGDM and extended correlated disorder model (ECDM) models cannot cope with the experimental observations in dynamic characterization (low-frequency rise in capacitance and variations in the current transients). Thus, charge carrier relaxation is accounted for in a multiple-trapping and release (MTR) model, see Ref. 17, where the conduction energy level, DOS shape, capture, and release rate may be derived from a Monte Carlo (MC) simulation or from steady-state EGDM parameters.

The work of Weiss *et al.*[4] focuses on three measurements methods, namely, current-voltage curves, dark injection transient currents (DITC), and impedance spectroscopy (IS), with the overall goal to extract a consistent charge mobility for the three measurement techniques. However, the extracted mobility values vary for the different measurement and mobility extraction methods. The origin of the discrepancies is not fully understood. In this paper, we analyze these mobility determination methods by using a MTR model with a discrete trap level. This allows for a clear classification into slow and fast traps and shows their distinct behavior. In a more general Gaussian or exponential trap DOS, the coexistence of slow and fast traps is very likely so that their influence cannot be easily distinguished. We then compare the extracted charge mobility from DITC simulations with the values obtained from IS simulations. We also relate them to the charge mobility obtained from steady-state current-voltage curves.

In the second part of this manuscript, we focus on the dark injection transient currents of organic light-emitting devices (OLEDs). This method has been suggested by various authors[1,4,18,19] for the determination of charge mobility in organic semiconductors. While Ref. 4 claims that DITC is the most suitable method for thin samples, Esward *et al.*[20] have pointed out that dark injection transient current measurements of OLEDs are sensitive to a range of experimental parameters such as pulse on- and off-times. So far, the charge mobility values have been extracted from the current response measurements[1,4,18,19] by the formula $\mu = 0.786\frac{l}{\tau_{DI}E}$ (Ref. 21), where τ_{DI} is the dark injection peak time and l is the thickness of the device. Commonly used models, however, do not take into account relaxation effects such as charge trapping and are insensitive to on-and off-time effects. In this paper, we suggest the presence of shallow charge trap states in a hole-only device indicated by the slow current decay process and discuss the influence of different trap regimes on the dynamic device behavior.

II. PHYSICAL MODEL

First, we introduce the underlying physical model for the steady and transient case. A hole-only device is chosen to be in line with the experimental data of Ref. 20 which is used for a comparison in the second part of this manuscript. We assume an Ohmic contact on both electrodes. The model

a)Electronic mail: evelyne.knapp@zhaw.ch.
b)Electronic mail: beat.ruhstaller@zhaw.ch.

for the hole-only device consists of Poisson's equation (Eq. (1)) and the continuity equation (Eq. (3)) for holes. In the steady-state case, the derivative with respect to time in Eq. (3) is set to zero. Expressing the free charge carrier density with a subscript f and the trapped carrier density with t, we obtain the following system of equations:

$$\nabla \cdot (\epsilon \nabla \psi) = q(-p_f - p_t), \tag{1}$$

where the permittivity is denoted by ϵ, the elementary charge by q, and the potential by ψ. The drift-diffusion equation for holes reads

$$J_p = -q p_f \mu \nabla \psi - qD \nabla p_f \,, \tag{2}$$

with the diffusion constant $D = \frac{\mu kT}{q}$. Only free charges contribute to the current. The charge continuity equation is described by

$$q \frac{\partial p_f}{\partial t} = -\nabla \cdot J_p - q \frac{\partial p_t}{\partial t}. \tag{3}$$

In the steady-state, we assume quasi-equilibrium between free and trapped charges. We employ the multiple trapping and release model with a constant mobility and a Dirac-distribution for the trap density of states (discrete level of traps at E_t). The trapped charge carrier density can then be written as the integral over all energy states of the trap density of states multiplied with the Fermi-Dirac statistics. We obtain

$$p_t(E_t) = N_t / \left(1 + \exp\left(\frac{E_F - E_t}{kT}\right)\right), \tag{4}$$

where E_t denotes the energy level of a single hole trap state and E_F is the Fermi energy.

To simulate the transient current response, we use the kinetic equation for trapped charges

$$\frac{\partial p_t}{\partial t} = c_p p_f [N_t - p_t] - e_p p_t. \tag{5}$$

The parameter c_p is the capture coefficient and can be related to the hopping attempt frequency as used in Ref. 17 or further to the capture cross section as used in Refs. 5 and 22. The parameter e_p is the rate for escape. The lifetime of a charge in a trap state is described by $\tau_e = 1/e_p$. For the lifetime τ_c in the HOMO, we obtain $\tau_c = 1/(c_p[N_t - p_t])$.[23,24] Further, the value of N_t denotes the number of trapping sites. The capture coefficient c_p is chosen and the escape rate e_p is given by $e_p = c_p N_0 \exp\left(\frac{E_v - E_t}{kT}\right)$ depending on the energetic depth of the trap and the capture coefficient. The number of sites for free holes is denoted by N_0, the parameter E_v stands for the HOMO level. In Table I, the parameters used in the simulations are listed. The above equations are solved in the numerical framework of Ref. 25 with an extension for transient simulations. To solve the coupled system of stiff equations, we use the implicit Euler method with adaptive time stepping.

III. CLASSIFICATION OF TRAPS

First, we classify traps in the steady-state, and then we extend the analysis to transient simulations such as impedance spectroscopy and dark injection transient currents. In the steady-state, two types of traps can be observed: deep and shallow traps. In Fig. 1, the charge trap regimes for holes are visualized with respect to the Fermi energy which separates deep and shallow traps. When the applied voltage is increased, then the deep states are being filled and correspondingly, the steepness of the current voltage curve is affected. The shallow traps are located below the Fermi energy and do not change the steepness of the current-voltage but reduce the current density. The occupation function $1 - f(E)$ for holes is shown in Fig. 1 (not to scale). Shallow traps can be split into fast and slow traps depending on the capture coefficient c_p. By choosing a discrete trap level in the shallow regime and varying the capture coefficient c_p we can either get fast or slow charge traps.

TABLE I. Simulation parameters of the hole-only device.

Name	Parameter	Value	Units
Number of sites	N_0	8.5×10^{26}	m^{-3}
Charge mobility	μ	5.6^{-10}	$m^2V^{-1}s^{-1}$
Charge density at anode	$p(0)$	$0.5 \times N_0$	m^{-3}
Charge density at cathode	$p(l)$	$0.5 \times N_0$	m^{-3}
Device thickness	l	205×10^{-9}	M
Number of trap sites	N_t	10^{23}	m^{-3}
Energetic trap level	E_t	0.2	eV
Built-in potential	V_{bi}	0	V
Capture coefficient	c_p	10^{-20}	m^3s^{-1}

A. Current-voltage curves

In the following sections, we use the device configuration of Table I and study the influence of a discrete level of traps at E_t. The results, however, are analogous for more general trap density of states. We now simulate two current-voltage curves, once with and without traps as shown in the inset of Fig. 2 in the regime of 0.1 V to 20 V. Shallow traps reduce the current-density but do not change the steepness of the current-voltage curve. Thus, they are parallel. At higher

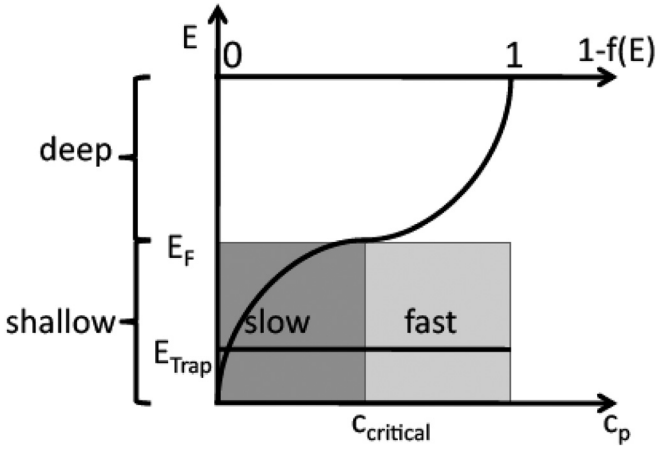

FIG. 1. The classification of hole charge traps into deep and shallow trap states depends on the Fermi energy and the filling of trap states on the occupation function $1 - f(E)$. The charge trap dynamics allows a further classification into fast and slow shallow traps.

voltage, the two curves will eventually merge when the traps are filled. In order to analyze the influence of shallow traps on the extraction of charge carrier mobility from current voltage curves, we now apply Mott-Gurney's formula to get

$$\mu = J/(9/8\epsilon(V - V_{bi})^2/l^3) \tag{6}$$

and extract the mobility values from the two curves as displayed in Fig. 2. In the trap-free case, the extracted mobility values at low voltages are far from the reference mobility μ that was used in the simulation. This is due to the diffusion current in Eq. (2) that dominates at low voltage. As expected, with increasing voltage the agreement between the extracted and the reference mobility improves. The diffusion current is neglected completely in Mott-Gurney's formula. The relation between the extracted mobility for the trap-free case and the one with traps is in good agreement with the reference mobility μ and the theoretically predicted value $\theta\mu$, where the parameter θ is the fraction of free charge carriers with respect to the total carriers,

$$\theta = \frac{p_f}{p_f + p_t}, \tag{7}$$

as originally analyzed by Rose.[26] To calculate the value of the parameter θ, we used the average charge densities in the bulk of the device. The absolute values of the carrier mobilities, however, are overestimated due to the diffusion current.

B. Impedance spectroscopy

We now turn to a dynamic charge transport characterization technique, the impedance spectroscopy that has become more popular recently. In impedance spectroscopy, a voltage modulation $V = V_0 + V^{ac}\exp(i\omega t)$ is applied to the device on the working point V_0 and the current response I^{ac} is monitored for different excitation frequencies ω. Thereof the complex admittance or impedance can be calculated: $Y = \frac{1}{Z} = \frac{I^{ac}}{V^{ac}} = G(\omega) + i\omega C(\omega)$, where G is the conductance, C is the capacitance, f is the frequency, and $\omega = 2\pi f$ is the angular frequency. To determine the charge mobility from impedance measurements Martens *et al.*[6] suggested analyzing the negative differential susceptance $-\Delta B = -\omega(C(\omega) - C_0)$ as a function of frequency where C_0 describes the geometric capacitance. The frequency f_{max} corresponding to the maximum of $-\Delta B$ is linked to the transit time t_{tr} of the carriers and thus to the mobility

$$\mu = 1.85\frac{f_{max}l^2}{(V - V_{bi})}. \tag{8}$$

This method in combination with trap kinetics in semiconductor devices has been studied by Montero *et al.*[27] and earlier by Refs. 28 and 29. The influence of slow and fast traps can be looked at in impedance spectroscopy since it is a suitable method for detecting relaxation processes in the charge transport at different time scales. We analyze the influence of slow and fast traps on the capacitance vs. frequency curve, see Fig. 3 (top). For the slow traps, the repeated trapping and de-trapping of charge carriers cause an increased capacitance at low frequency. At higher frequency, de-trapping is slower than the voltage modulation and we obtain the same value as in the trap-free case. Slow traps enhance the capacitance at low frequency as shown in Fig. 3 and fast traps shift the capacitance step to lower frequencies indicating a lower charge mobility value.[27,30,31] On the bottom of Fig. 3, we show the negative differential susceptance for slow and fast traps as well as the trap-free case. We indicate the maximum value of $-\Delta B$ in the plot and extract the mobility values thereof with the help of Eq. (8). Slow traps alter the low frequency end of the plot, while fast traps change the peak position of the differential susceptance. The difference in the apparent mobility in the fast trap case compared to the trap-free case is again in accordance with the parameter θ as is shown further below.

C. Dark injection transient currents

Further, we extend the above studies to dark injection transient current technique which is, in contrast to the IS technique, a large signal perturbation, since dark injection

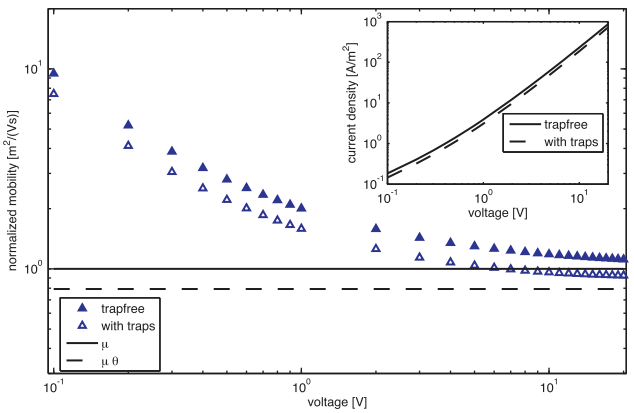

FIG. 2. In the inset steady-state current-voltage curves for the trap-free case and with traps are plotted. We compare the thereof extracted charge mobilities with the reference mobility μ and the effective mobility μ_{eff}.

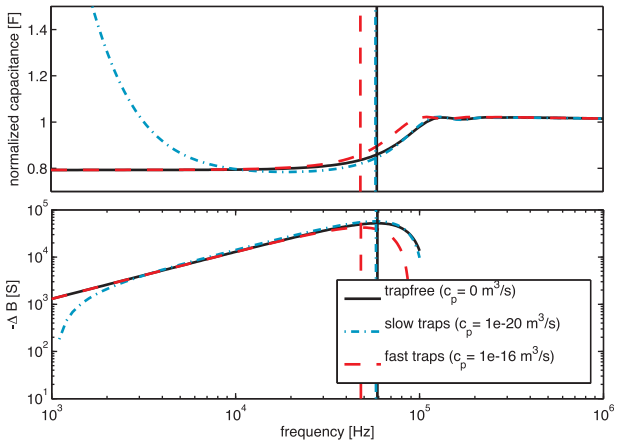

FIG. 3. Top: the enhanced capacitance at low frequency for slow traps and the shift of the capacitance step for fast traps is shown. As a reference, the trap-free case is plotted. Bottom: to extract the mobility the maximum of the negative differential susceptance is determined for the slow, fast, and trap-free cases.

transient currents are the response to a large voltage step. The DITC technique is frequently also called transient space-charge-limited current (T-SCLC) technique. First, we look at slow traps, i.e., we choose a small capture coefficient c_p and apply a step voltage of 8 V to the hole-only device in equilibrium as shown in Fig. 4. The peak of the current response remains at the same position on the time axis, denoted by τ_{DI}, as for the trap-free case and we can apply the analytical formula

$$\mu = 0.786 \frac{l^2}{\tau_{DI}(V - V_{bi})}. \tag{9}$$

By using different values for the capture coefficient c_p the decay after the peak position of the current can be influenced. For a higher capture coefficient and thus faster trapping mechanism the peak position shifts. It is notable that beyond a certain capture rate, the peak position τ_{DI} does not shift any further. As a limit, we reach the quasi-equilibrium between free and trapped charge carriers. Further, the trap-free current density in the steady-state limit is reduced by a factor θ in case of trapping in agreement with Fig. 2. Depending on the capture coefficient c_p, the transient current decays to the steady-state current density shortly after the peak position (fast traps) or strongly delayed (slow traps). For instance, in Fig. 4, the transient current in the example of slow traps reaches the steady-state value only after two orders of magnitude on the time scale.

Charge traps can be classified according to their escape rate and capture rate with respect to their transit time t_{tr}. We use, therefore, the mean lifetime of the free carrier in the HOMO τ_c and the lifetime in the trap τ_e. If the trap relaxation time τ_{relax} given by $1/\tau_{relax} = 1/\tau_c + 1/\tau_e$ (Ref. 24) is significantly smaller than the transit time t_{tr}, we deal with fast traps and see a shift in the peak position τ_{DI} since all charge carriers are being repeatedly trapped and released when traveling through the device, thus effectively increasing the transit time and lowering the mobility. If time τ_{relax} is greater than the transit time t_{tr}, then the relaxation process is slower than the crossing for holes and thus only visible in the slow decay after the current peak. The charge mobility is then identical to the trap-free case.

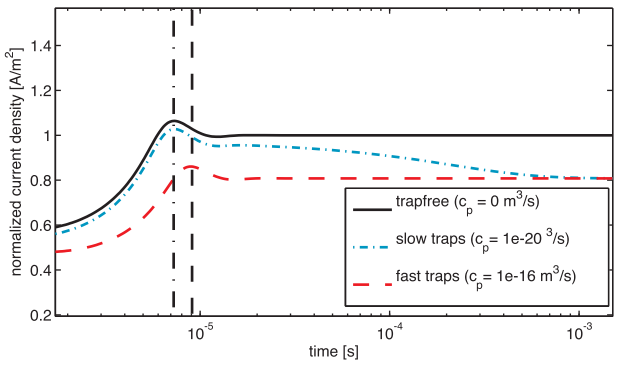

FIG. 4. DITC simulation results for the slow, fast, and trap-free cases are displayed. A shift of the peak position is observed for fast traps while slow traps cause a slow decay of the current density after the peak position.

D. Mobility from dynamic characterization

Next, we summarize the above findings with respect to mobility determination from the simulated (rather than experimental) curves. In Fig. 5, we extract the charge mobility values from the IS and DITC simulations for different capture coefficients c_p according to the formulas (8) and (9). We find the maximum of the negative differential susceptance for the calculated frequencies in the IS case and the peak position of the current response for the discrete time steps in the DITC case. We also plotted the reference mobility of the free carriers which is used as input parameter for the simulations. Further, the effective mobility in the presence of traps $\mu_{eff} = \theta\mu$ is also displayed. For small capture coefficients, the trap states act as slow traps and the extracted mobility corresponds to the reference mobility. By increasing the capture coefficient c_p, we get fast traps and the extracted mobility is in good agreement with the effective mobility $\mu_{eff} = \theta\mu$. The critical capture coefficient c_{crit} which separates the two regimes (slow and fast) can be determined from the comparison of the relaxation and transit time $\tau_{rel} \approx t_{tr}$ in the DITC case and in the IS case as described in Ref. 27. The two critical capture coefficients are indicated as vertical lines in Fig. 5. It is remarkable that both dynamic characterization techniques, IS and DITC, suffer from the same ambiguities when it comes to determining charge mobilities from them.

The model presented in this paper can likely explain different charge mobility values extracted from SCLC current-voltage curves and DITC or IS data as reported by Weiss *et al.*[4] For instance, let us assume a device with trap states. From the current voltage curve, we obtain an effective mobility $\mu_{eff} = \theta\mu$ whereas from DITC and IS measurements the mobility μ is extracted in case of slow trapping. Slow trapping can, therefore, explain the discrepancy in extracted mobility values from current voltage-curves, IS and DITC. Slow and fast trapping cannot be distinguished in the steady-state, only dynamic characterization reveals two different regimes in our model calculations. While slow traps result in characteristically modified IS and DITC curves (capacitance vs. frequency curve increases at low frequencies—DITC decays on a long time scale), fast traps lead to curves that are qualitatively similar to the trap-free case.

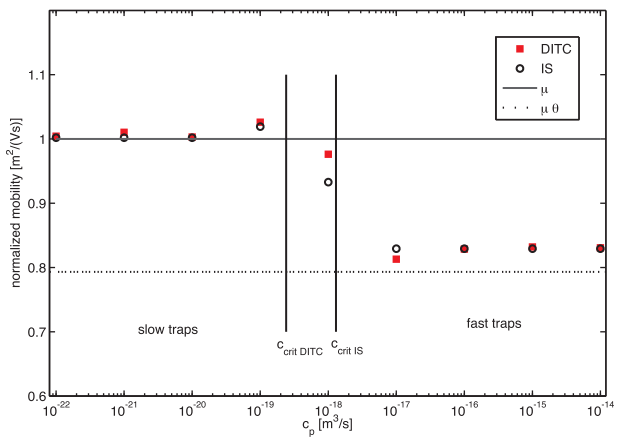

FIG. 5. Extracted mobility values from DITC and IS for different capture coefficients. The reference mobility μ is an input parameter for the simulation.

IV. ANALYSIS OF CURRENT PULSE SEQUENCE

In the last part of this paper, we aim at elucidating the impact that trapped charges may have on repetitive pulsing as it is typically used in measurements. It is common to acquire the pulse shape with an oscilloscope in averaging mode. In Ref. 20, a systematic study on the sensitivity of single carrier transport to changes in the applied voltage pulse is performed. Experimental parameters such as the pulse amplitude, on-time, off-time, and the ambient temperature were varied. In this paper, we focus on the observation that the charge mobility values extracted from the measurements vary with the pulse off-time. We show the simulation results for a trap-free device and one with a shallow discrete trap level. We perform the simulation for a sequence of pulses in order to assess possible relaxation effects. For the case with a discrete trap level, we indeed observe that the transient current response varies for the initial pulses before becoming periodic. Obviously, the device cannot recover to the initial state during the off-period of the pulse. In Fig. 6, we show several cycles of the DITC simulation. In the trap-free case, all periods are identical because the on- and off-times are long enough for the device to reach the steady-state. For the device with traps, we eventually obtain a slow decay after the current peak and a reduced current at the end of the period of the pulse with respect to the trap-free case. Only after a few cycles, the pulse transients become periodic. In the trap-free case, we cannot reproduce the slow decay after the peak position nor the shift of the peak position with the off-time variation (see Ref. 20) since the device returns quickly to its initial state during the off-time as there are no charges being trapped and released.

We repeat the pulse sequence calculations in Fig. 6 for different off-times and plot the current pulse in Fig. 7, as it settles after a few periods. We calculate the transient current as a function of the duty cycle which is defined as the fraction of on-time to the total pulse period. The thick red line (66%) corresponds to the calculation with traps shown in Fig. 6. By increasing the off-time, i.e., decreasing the duty cycle, the current density at the peak position is enhanced since the device is almost reaching its initial state during the off period. With shorter off-times, the current density is reduced and the peak position slightly shifted. Note that this shift of the peak position on the time axis with decreasing off-time leads to a higher value of τ_{DI}, thus to a lower effective mobility value. This observation is in agreement with the DITC experiments of Ref. 20 where different apparent charge mobility values are extracted for different off-times. With the trap kinetics in the numerical model, we found a suitable and convincing explanation for the observed relaxation effects in DITC measurements in OLEDs.[20]

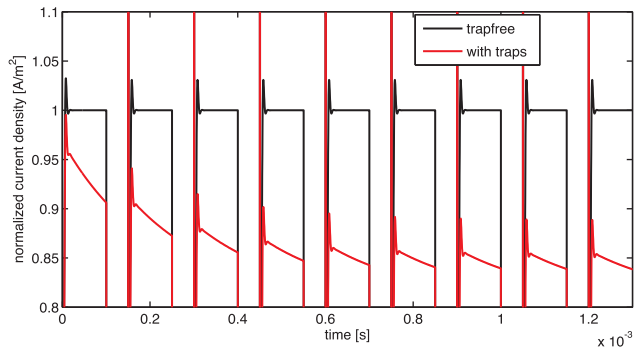

FIG. 6. We show pulse sequences of a device with and without trapping. The trap-free devices reach its steady-state value during the on-time as well as during the off-time. This is not the case if traps are present.

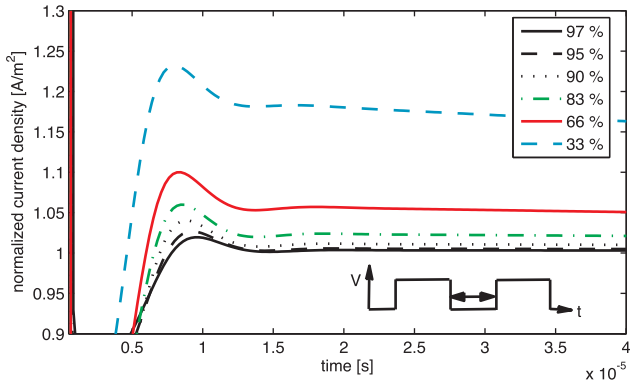

FIG. 7. The inset shows the input signal of the applied voltage over time. The off-time is varied by applying different duty cycles to the device. Note the shift of the peak position towards longer times for higher duty cycles.

V. CONCLUSIONS

For shedding light on discrepancies among commonly performed electrical characterization techniques for charge mobility determination, we have employed a numerical drift-diffusion model that includes charge traps. We have investigated charge mobility determination methods based on current-voltage, IS, and DITC simulations with trap states. The presence of traps leads to a reduced current or an increased steepness in the steady-state current-voltage curve. The classification in fast and slow traps is an important step in the analysis of the transient data. Depending on the capture coefficient c_p two different mobility values can be extracted in the transient characterization of a device, namely, the reference mobility μ and the effective mobility $\mu_{eff} = \theta\mu$. Our model thereby will allow for a consistent description of different measurement techniques and help to avoid ambiguities in the interpretation of experimental data. Therefore, we have modeled both small signal as well as large signal perturbation techniques. Further, we have used our model with charge traps for DITC simulations, and it is able to reproduce the slow decay of the current peak and the shift of the peak position as commonly observed in DITC experiments such as presented in Ref. 20. This extended model is thus capable of generating more realistic current transients and may help to reveal crucial parameters of charge traps such as density, energetic depth, and the capture coefficient. The presented model can be extended to continuous trap distributions as opposed to a single trap level.

ACKNOWLEDGMENTS

We acknowledge financial support from the European Community's Seventh Framework program under Grant Agreement Nos. 213708 (www.AEVIOM.eu) and NMP4-SL-2011-295368 (www.im3oled.eu).

[1]D. Poplavskyy and J. Nelson, J. Appl. Phys. **93**, 341 (2003).
[2]D. Poplavskyy, W. Su, and F. So, J. Appl. Phys. **98**, 014501 (2005).
[3]D. Poplavskyy and F. So, J. Appl. Phys. **99**, 033707 (2006).
[4]O. J. Weiss, R. K. Krause, and A. Hunze, J. Appl. Phys. **103**, 043709 (2008).
[5]T. Okachi, T. Nagase, T. Koboyashi, and H. Naito, Jpn. J. Appl. Phys., Part 1 **47**, 8965–8972 (2008).
[6]H. C. F. Martens, H. B. Brom, and P. W. M. Blom, Phys. Rev. B **60**, R8489 (1999).
[7]H. C. F. Martens, J. N. Huiberts, and P. W. M. Blom, Appl. Phys. Lett. **77**, 1852 (2000).
[8]H. C. F. Martens, W. F. Pasveer, H. B. Brom, J. N. Huiberts, and P. W. M. Blom, Phys. Rev. B **63**, 125328 (2001).
[9]S. W. Tsang, S. K. So, and J. B. Xu, J. Appl. Phys. **99**, 013706 (2006).
[10]W. F. Pasveer, J. Cottaar, C. Tanase, R. Coehoorn, P. A. Bobbert, P. W. M. Blom *et al*. Phys. Rev. Lett. **94**(20), 206601 (2005).
[11]S. L. M. van Mensfoort, S. I. E. Vulto, R. A. J. Janssen, and R. Coehoorn, Phys. Rev. B **78**, 085208 (2008).
[12]S. L. M. van Mensfoort, J. Billen, S. I. E. Vulto, R. A. J. Janssen, and R. Coehoorn, Phys. Rev. B **80**, 033202 (2009).
[13]B. Ruhstaller, S. A. Carter, S. Barth, H. Riel, W. Riess, and J. C. Scott, J. Appl. Phys. **89**, 4575 (2001).
[14]B. Ruhstaller, T. Beierlein, H. Riel, S. Karg, J. C. Scott, and W. Riess, IEEE J. Sel. Top. Quantum Electron. **9**, 723 (2003).
[15]C. Pflumm, C. Grtner, and U. Lemmer, IEEE J. Quantum Electron. **44**, 790–798 (2008).
[16]J. Rogel-Salazar, D. D. C. Bradley, J. R. Cash, and J. C. deMello, Phys. Chem. Chem. Phys. **11**, 1636–1646 (2009).
[17]W. Chr. Germs, J. J. M. van der Holst, S. L. M. van Mensfoort, P. A. Bobbert, and R. Coehoorn, Phys. Rev. B **84**, 165210 (2011).
[18]J. C. Scott, S. Ramos, and G. G. Malliaras, J. Imaging Sci. Technol. **43**, 233 (1999).
[19]A. J. Campbell, D. D. C. Bradley, and H. Antoniadis, J. Appl. Phys. **89**, 3343 (2001).
[20]T. Esward, S. Knox, H. Jones, P. Brewer, C. Murphy, L. Wright, and J. Williams, J. App. Phys. **109**, 093707 (2011).
[21]A. Many and G. Rakavy, Phys. Rev. **126**, 1980 (1962).
[22]J. Staudigel, M. Stössel, F. Steuber, and J. Simmerer, J. App. Phys. **86**, 3895 (1999).
[23]D. Dascalu, Solid-State Electron. **9**, 1020 (1966).
[24]D. Dascalu, Solid-State Electron. **11**, 491 (1968).
[25]E. Knapp, R. Häusermann, H. U. Schwarzenbach, and B. Ruhstaller, J. Appl. Phys. **108**, 054504 (2010).
[26]A. Rose, *Concepts in Photoconductivity and Allied Problems* (John Wiley and Sons, 1963).
[27]J. M. Montero, J. Bisquert, G. Garcia-Belmonte, E. M. Barea, and H. J. Bolink, Org. Electron. **10**, 305 (2009).
[28]D. Dascalu, Int. J. Electron. **21**, 183 (1966).
[29]R. Kassing, Phys. Status Solidi A **28**, 107 (1975).
[30]E. Knapp and B. Ruhstaller, Appl. Phys. Lett. **99**, 093304 (2011).
[31]E. Knapp and B. Ruhstaller, Opt. Quantum Electron. **42**, 667 (2011).